

DESY 92-017
CERN-TH.6403/92
FTUAM-EP/92-04
May 1992

DESY-Bibliothek

Elastic and Diffractive Photoproduction of J/ψ Mesons

G. A. Schuler

CERN, THEORY DIVISION, GENEVA, SWITZERLAND

J. Terron

Deutsches Elektronen-Synchrotron DESY, Hamburg

ISSN 0418-9833

Elastic and Diffractive Photoproduction of J/ψ mesons

Gerhard A. Schuler

Theory Division, CERN
CH-1211 Geneva 23
Switzerland

Juan Terron^{a,b}

Deutsches Elektronen Synchrotron – DESY
Notkestr. 85, 2000 Hamburg 52, Germany

Abstract

We propose models for elastic and diffractive J/ψ production based on pomeron exchange and vector-meson dominance. The production mechanisms are compared with results from fixed target photo- and muoproduction experiments. This includes integrated cross sections as well as differential distributions. We investigate the overlap of diffractive J/ψ production with inelastic production as modelled in the colour singlet model. When properly adding both contributions, we can explain the excess of events seen at large $z = E_{J/\psi}/E_\gamma$. Using the energy dependence of the respective models, predictions for elastic, diffractive and inelastic J/ψ production at the electron-proton collider HERA are made.

^aOn leave of absence from Dpto de Fisica Teorica, Univ. Autonoma de Madrid, Spain.

^bPartially supported by the exchange programme CICYT-Kfz., Karlsruhe.

•

•

High-energy, small-momentum-transfer processes are successfully described within the picture of pomeron and reggeon exchange [1]. The basic and intriguingly simple properties of the pomeron have been established by studying various soft hadronic reactions; they allow a faithful description of available data without resorting to unknown dynamics. The link with QCD still remains to be done but, given the phenomenological success, we attempt to apply the idea of pomeron exchange to the photoproduction of J/ψ mesons.

Our starting point is the description of elastic and total (anti-)proton-proton cross sections, as well as diffractive proton dissociation $pp \rightarrow pX$, by Landshoff et al. [2, 3]. They assume that the pomeron is an isolated Regge pole with a residue that factorizes. Moreover, it couples to single quarks like a $C = +1$ isoscalar photon. Using the additive-quark rule following from these assumptions, allowing for a different coupling to charm quarks and modelling the form factor of the J/ψ meson, we apply these ideas to J/ψ proton scattering. The concept of vector-meson dominance is then used to establish the link to photoproduction of J/ψ mesons. In this way we describe elastic scattering, $\gamma + p \rightarrow J/\psi + p$.

The assumption that the pomeron couples rather like the photon can be extended to the inelastic processes. This allowed Landshoff et al. to calculate diffractive proton dissociation in terms of the structure function νW_2 that is measured in lepton scattering [3]. It is worth noting that the description is remarkably successful over a wide range in t , without requiring any new parameters. We extend these ideas to photoproduction of J/ψ via diffractive dissociation (DD) of the proton¹, $\gamma + p \rightarrow J/\psi + X$.

The DD process differs from inelastic J/ψ production in that the J/ψ is separated from the remaining hadronic system by a large rapidity gap. In photoproduction experiments J/ψ events could be classified as elastic or DD events if no charged or neutral track accompanied the J/ψ [4, 6, 7]. In muoproduction, events are labelled as “elastic” if the energy deposit in the calorimeter is less than ~ 5 GeV (BFP [8]) or if the inelasticity variable $z = E_{J/\psi}/E_\gamma$ is above a cut, $z \geq 0.95$ for EMC [9], $z \geq 0.90$ for NMC [10]. The experimental input to this letter is listed in Table 1.

Typically, the momentum transfer t between the photon and the J/ψ is small for the DD process and even smaller for elastic J/ψ production. As the momentum transfer and/or the mass of the remaining hadronic system X increases, the diffractive reaction is expected to change into inelastic J/ψ production. At sufficiently large t or M_X , inelastic J/ψ production can be calculated perturbatively, using the so-called colour-singlet (CS) model [11]. The relevant subprocess, $\gamma + g \rightarrow J/\psi + g$, is a direct probe of the gluon density of the proton. This fact was exploited by the NMC [10] to determine the gluon distribution of the proton. Inelastic J/ψ production is also suggested as a tool to extract the gluon density in ep collisions at HERA, in particular at small x values [5]. To this end it is of crucial importance to estimate the validity range of the CS model and to study its transition to the DD process. This question we address in the last part of this letter.

The afore-mentioned properties of the pomeron led to the following form of the proton-proton elastic amplitude [2]

$$T = i (3\beta F_1(t))^2 (\alpha' s)^{\sigma p(t)-1}, \quad (1)$$

where $\beta^2 = 4 \text{ GeV}^{-2}$ describes the pomeron coupling to light quarks and $F_1(t)$ is the isoscalar

¹To be distinguished from diffractive photon dissociation, $\gamma + p \rightarrow (J/\psi + X) + p$, which has a much smaller cross section [4, 5].

| E_γ [GeV] | σ [nb] | | | Slope: $d\sigma/dt \sim \exp(bt + ct^2)$ or $\exp(-B_1 p_T^2) + \kappa \exp(-B_2 p_T^2)$ | | |
|-------------------------|----------------|---------------|----------------|---|----------------------|--|
| | Elastic | DD | Sum | Elastic | DD | Sum |
| IF [7] 100 GeV | 15.7 ± 3.1 | 6.8 ± 1.4 | 22.5 ± 4.5 | $b = 5.6 \pm 1.2$ $c = 2.9 \pm 1.3$ | | |
| FTPS [4] 105 GeV | 9.8 ± 2.0 | 4.4 ± 1.4 | 14.2 ± 2.1 | | | |
| NA14 [6] 100 GeV | | | 14.0 ± 3.0 | | | $B_1 = 2.5 \pm 0.2$ $B_2 = 0$ |
| BFP [8] 108 GeV | | | 20.7 ± 1.2 | | | |
| EMC [9] 100 GeV | | | 12.2 ± 2.0 | | | $B_1 = 5.2 \pm 0.6$ $B_2 = 0.66 \pm 0.14$ |
| NMC [10] 100 GeV | | | 12.7 ± 2.0 | | | $b = 1.2 \pm 0.1$ $c = 0$ |
| Model 100 GeV | 9.8 | 2.8 | 12.6 | $b = 4.3$ $c = 0$ | $b = 1.7$ $c = 0$ | $b = 2.4$ $c = 0$ |
| $\sqrt{s} =$ 250 GeV | 17.5 | 10.3 | 27.8 | $b = 7.2$ $c = 0$ | $b = 2.5$ $c = 0$ | $b = 2.6$ $c = 0$ |

Table 1: Cross sections and slope parameters for elastic and diffractive J/ψ production, $\gamma N \rightarrow J/\psi + p$, $J/\psi + X$. For FTPS ($N = p$), elastic means forward elastic and rear elastic, DD means forward elastic and rear inelastic. For IF ($N = H, D$), elastic means elastic, DD means diffractive target dissociation. For NA14 ($N = {}^6\text{Li}$), sum means elastic (forward elastic). The errors for the photoproduction experiments include statistical and systematic errors. For BFP muoproduction ($N = \text{Fe}$), elastic means ECAL < 5 GeV with corrections. For EMC muoproduction ($N = \text{Fe}$), contribution from ψ' not removed, smearing corrections not made, sum means: $z > 0.95$. For NMC muoproduction ($N = H, D$), contribution from ψ' not removed, sum means: $z > 0.90$.

Dirac form factor: $F_1(t) = (1 - 2.79\tau)(1 - \tau)^{-1}(1 - t/0.71 \text{ GeV}^2)^{-2}$, where $\tau = t/(4m_p^2)$. The trajectory was found to be rather linear: $\alpha_P(t) = 1 + \epsilon + \alpha' t$, where $\alpha' = 0.25 \text{ GeV}^{-2}$ and $\epsilon = 0.085$. The value of ϵ is in accordance with the observed rise of the proton-antiproton cross section up to Tevatron energies [1].

In the following we only take into account the single-pomeron-exchange contribution and neglect double- and multiple-pomeron-exchange contributions. There is no contribution from Reggeon exchange to J/ψ proton scattering as is the case for (anti-)proton-proton scattering since this contribution is associated with the exchange of valence quarks. Therefore we did not include it in (1). Double- and multiple-pomeron-exchange contributions become more important at higher energy. Yet, experience from pp elastic scattering shows that these may be neglected at present energies, presumably up to maximal HERA energies, $\sqrt{s_{pp}} \approx 250 \text{ GeV}$.

It is straightforward to obtain the differential cross section for elastic pp scattering from (1):

$$\frac{d\sigma^{\text{el}}(pp)}{dt} = \frac{|T|^2}{4\pi} = \frac{1}{4\pi} (3\beta F_1(t))^4 (\alpha' s)^{2(\epsilon + \sigma' t)}. \quad (2)$$

From the imaginary part of the amplitude, one obtains the total cross section:

$$\sigma^{\text{tot}}(pp) = 2 \text{Im}(T)|_{t=0} = 18\beta^2 (\alpha' s)^\epsilon. \quad (3)$$

The above picture of pp elastic scattering can easily be generalized to J/ψ proton elastic scattering. The corresponding expression for $J/\psi + p \rightarrow J/\psi + p$ (see Fig. 1a) can be inferred from (2) by changing the square of one of the proton elastic form factors to the square of the J/ψ elastic form factor. Correcting also the constant factor related to the different number of quarks in the proton and in the meson we arrive at

$$\frac{d\sigma^{\text{el}}(J/\psi p)}{dt} = \frac{1}{4\pi} (3\beta F_1(t))^2 (2\beta' F_{J/\psi}(t))^2 (\alpha' s)^{2(\epsilon + \sigma' t)}. \quad (4)$$

In Eq. (4) we allow for a different coupling of the pomeron to the charm quarks of the meson, β' instead of β , which quantifies the coupling to light quarks. The missing link to γp scattering is finally established by invoking vector-meson dominance:

$$\frac{d\sigma^{\text{el}}(\gamma p \rightarrow J/\psi p)}{dt} = \frac{4\pi\alpha}{f_{J/\psi}^2} \frac{d\sigma^{\text{el}}(J/\psi p)}{dt}, \quad (5)$$

where we take $4\pi\alpha/f_{J/\psi}^2 = 1/1570$ [12].

We make the following ansatz for the J/ψ form factor valid at sufficiently small $|t|$:

$$F_{J/\psi}(t) = \exp(B_{J/\psi} t). \quad (6)$$

Furthermore we assume that the slope parameter B_H for the elastic form factor of a hadron H scales like the squared radius of that hadron. This gives us: $B_{J/\psi} = B_p r_{J/\psi}^2/r_p^2$. As the J/ψ radius, $r_{J/\psi}$ is about one third [13] of the proton radius, r_p , we obtain $B_{J/\psi} \sim 10\% B_p \sim 0.23 \text{ GeV}^{-2}$. At small- t the t -distribution of (5) can be written as

$$\frac{d\sigma^{\text{el}}}{dt} \approx \frac{d\sigma^{\text{el}}}{dt} \Big|_{t=0} \exp\{B_{\text{el}} t\}, \quad (7)$$

where

$$B_{\text{el}} = 2B_p + 2B_{J/\psi} + 2\alpha' \log(\alpha' s) \\ \frac{d\sigma^{\text{el}}}{dt} \Big|_{t=0} = \frac{4\pi\alpha}{f_{J/\psi}^2} \frac{9}{\pi} (\beta')^2 \beta^2 (\alpha' s)^{2\epsilon}. \quad (8)$$

In the following we use (6) for the J/ψ form factor, with $B_{J/\psi}$ as given above at all t but use $F_1(t)$ for the proton form factor. When considering the extended t range $0.25 < -t < 2 \text{ GeV}^2$, a value $B_p \approx 1.09$ would be more appropriate than the value 2.37 which is valid at small t . We note that the effect of the J/ψ form factor on the t slope is rather small, about 5–7% for the energies considered in this paper.

The integration of (5) over t is straightforward and yields, at $E_\gamma = 100 \text{ GeV}$: $\sigma^{\text{el}}(\gamma p \rightarrow J/\psi p) = 879 (\beta')^2 \text{ nb GeV}^2$. We emphasize that all the parameters of the model in Eqs. (4) and (5) except β' are fixed. Based on this single parameter the model predicts the elastic $\gamma + p \rightarrow J/\psi + p$ cross section as a function of the c.m. energy. Two experiments, IF [7] and FTPS [4], were able to isolate the elastic reaction from diffractive and inelastic J/ψ production. Their elastic cross sections at $\sqrt{s_{\gamma p}} = 13.7 \text{ GeV}$ ($E_\gamma = 100 \text{ GeV}$) agree within the experimental errors, see Table 1. We chose to fix β' from the FTPS value and obtain $(\beta')^2 = 0.011 \text{ GeV}^{-2}$.

With this value for β' we obtain good agreement with the t slope as measured by the IF collaboration, cf. Table 1. They also measured the energy dependence of the elastic cross section in the range $E_\gamma = 60\text{--}300 \text{ GeV}$. In this range we can approximate their data by

$$\frac{d\sigma^{\text{el}}}{dt} \Big|_{t=0} = A \left(\frac{E_\gamma}{10 \text{ GeV}} \right)^a. \quad (9)$$

While $A = 20 \text{ nb}$ and $a = 0.17$ in our model, the data seem to prefer a stronger rise with energy, $A \sim 9\text{--}30 \text{ nb}$ and $a \sim 0.76\text{--}0.35$. In their analysis of the energy dependence of $d\sigma^{\text{el}}/dt$ the IF collaboration had to use the deuterium data since the hydrogen data were too weak statistically. The analysis is non-trivial since, besides effects such as inelastic contamination, energy dependence of the t distribution, etc., also the influence of the coherent peak in the deuterium data had to be studied. If the data were correct, it is still possible that present energies are too low yet for our ansatz to be valid. It will be very interesting to compare it with forthcoming data from HERA, where photon-proton cross sections will be measurable up to $\sqrt{s_{\gamma p}} \sim 250 \text{ GeV}$. Extrapolating naively the linear fit of the IF collaboration with an energy slope of $(0.1 \pm 0.02) \text{ nb/GeV}$ up to HERA energies yields $(3.2 \pm 0.6) \mu\text{b}$ for the sum of elastic and DD cross sections. Assuming further a constant fraction of elastic events ($\sim 70\%$ at IF energies [7]) this corresponds to an increase by a factor of 140. In contrast, in our model we do not expect a strong increase: less than a factor of 2 with respect to present data, cf. Table 1. In passing we note that the J/ψ nucleon cross section may be extracted from the elastic cross section:

$$\sigma(J/\psi + p \rightarrow \text{all}) = 0.9 s^\epsilon \text{ mb}. \quad (10)$$

Next we study diffractive J/ψ production via DD of the proton. Here the photon couples to an off-shell J/ψ meson which is put on-shell by diffractive scattering of the proton, which

breaks up. The J/ψ scatters quasi-elastically, i.e. at small t , and is isolated in rapidity. Again we start with the description by Landshoff et al. of the analogous reaction in pp scattering. They show [3] that the $pp \rightarrow pX$ data can successfully be described if the square of one of the elastic proton form factors in (2) is replaced by an integral over the inelastic form factor:

$$(3\beta F_1(t))^2 (\alpha' s)^{2(\alpha_P(t)-1)} \rightarrow \int \frac{dM^2}{M^2} \left(1 - \frac{M^2}{s}\right) \left(\frac{s}{M^2}\right)^{2(\alpha_P(t)-1)} \beta^2 \bar{F}_2(x, |t|). \quad (11)$$

Here t is the squared momentum transfer between the initial and final proton (the inelasticity of the interchanged pomeron) and M^2 is the invariant mass of the hadronic system resulting from the dissociation of the other incident proton (see Fig. 1b). The differential cross section for $pp \rightarrow pX$ is then

$$\frac{d\sigma^{DD}(pp)}{dt dM^2} = \frac{1}{4\pi M^2} (3\beta F_1(t))^2 (s/M^2)^{2\alpha_P(t)-2} \left(1 - \frac{M^2}{s}\right) \beta^2 \bar{F}_2(x, |t|). \quad (12)$$

The structure function \bar{F}_2 is related to the standard νW_2 deep inelastic scattering function in the following way:

$$\nu W_2(x, Q^2) = x(4/9(u + \bar{u}) + 1/9(d + \bar{d})) \implies \bar{F}_2(x, Q^2) = x(u + \bar{u} + d + \bar{d}). \quad (13)$$

The variables x and Q^2 are given by the expressions:

$$x = \frac{|t|}{M^2 + |t| - m^2}, \quad Q^2 = |t|. \quad (14)$$

The typical Q^2 values involved in Eq. (12) are smaller than a few GeV², above which standard parametrizations of structure functions are valid. We shall use the parametrization of [3]b:

$$\bar{F}_2(x, Q^2) = 3.99 x^{0.56} (1-x)^3 \left(\frac{Q^2}{Q^2 + 0.85}\right)^{0.44} + 0.68 x^{-0.08} (1-x)^5 \left(\frac{Q^2}{Q^2 + 0.36}\right)^{1.08}. \quad (15)$$

The parametrization (15) vanishes at $Q^2 = 0$, as is required by gauge invariance for the photon. Since such a behaviour is not expected for the pomeron, the pomeron-photon analogy will break down at $Q^2 = 0$. In fact, in Ref. [3]b it was shown that the pomeron amplitude requires the last term in (15), $(Q^2/(Q^2 + 0.36))^{1.08}$, to be about 0.2 at $Q^2 = 0$ to fit the pp data. When using (15), our predictions for the DD process might thus fall below the data at very small t values and also result in a somewhat too small total rate. In Ref. [3]b a corrected formula was proposed for the DD process. This correction factor should not be applied here since it takes into account the contribution of the f meson which does not couple to the J/ψ .

The expression analogous to (12) for the process $\gamma + p \rightarrow J/\psi + X$ (Fig. 1c) is readily established:

$$\frac{d\sigma^{DD}(\gamma p \rightarrow J/\psi X)}{dt dM^2} = \frac{4\pi\alpha}{f_{J/\psi}^2} \frac{1}{4\pi M^2} [2\beta' F_{J/\psi}(t)]^2 \left(\frac{s}{M^2}\right)^{2\alpha_P(t)-2} \left[1 - \frac{M^2}{s}\right] \beta^2 \bar{F}_2(x, Q^2). \quad (16)$$

We emphasize that (16) is a zero-parameter model. To ensure that the pomeron is the predominant exchange, we impose the following cuts on the kinematical variables t and M^2 [3]b:

$$|t| < 2 \text{ GeV}^2, \quad (m_p + m_\pi)^2 < M^2 < 10\% s. \quad (17)$$

In Table 1 we compare the integrated DD process (16), as well as its sum with the elastic process (5), with data. Both the elastic and the DD rate of the IF collaboration [7] are larger than our predictions. On the other hand, the DD rate falls only slightly below the FTPS data whose elastic cross section we used to determine β' . This underestimation is expected from the afore-mentioned wrong low Q^2 behaviour of \bar{F}_2 . Yet, the difference is within the experimental error. We find similarly good agreement with data from NA14 [6], EMC [9] and NMC [10] for the sum of the elastic and DD process.

In Fig. 2 we compare the t distributions of elastic J/ψ production and J/ψ production via diffractive target dissociation at $E_\gamma = 100 \text{ GeV}$. We also show the t distribution of the sum of the two processes. The diffractive reaction has a much flatter slope, so that the slope of the elastic process is reduced by a factor of about 2 when including diffractive J/ψ production. In fact, the slope of the sum agrees nicely with the NA14 [6] measurement, as can be seen in Table 1 where we give the values of the slopes that we obtain when fitting the different t distributions of Fig. 2 in the range $0.25 \text{ GeV}^2 < -t < 2 \text{ GeV}^2$. The NA14 collaboration defines "elastic" scattering by the requirement that no charged or neutral track accompanies the J/ψ (called "beam elastic" events by FTFS [4]). This definition precisely includes elastic scattering as well as diffractive target dissociation. The results from muonproton are not directly comparable, since they could define "elastic" scattering only through a cut on $z = E_{J/\psi}/E_\gamma$, cf. Table 1. Then certain fractions of inelastic events are included. For a more precise comparison, the cuts (17) should be applied also to the data. Ideally, one would like to confront the two-fold differential distribution (16) with data.

In Fig. 3 we compare the energy dependence of beam elastic J/ψ production (i.e. elastic plus DD production) with various data. The observation is similar to that of elastic J/ψ production: The data seem to prefer a steeper increase than predicted by the model. Linearly extrapolating the low-energy data up to maximal HERA energy results in a very large cross section: $\sigma \sim O(\mu\text{b})$ at $\sqrt{s_{pp}} = 250 \text{ GeV}$. This is to be compared with the modest increase to 28 nb in our model, cf. Table 1.

We finally address the question of how diffractive J/ψ production is connected to inelastic J/ψ production. This question is important since the latter process has attracted interest as a way to extract the gluon distribution of the proton [5, 10]. The optimism is based on the assumption that this process can be calculated in perturbative QCD using the colour singlet (CS) model [11]. Here J/ψ production proceeds via the subprocess $\gamma + g \rightarrow c\bar{c} + g$ where colour and spin constraints of the J/ψ are imposed on the $c\bar{c}$ system. The latter is treated non-relativistically as an S-wave system and transformed into the J/ψ using its wave function at the origin. This wave function can be deduced from the measured leptonic decay width of the J/ψ .

The CS model is able to reproduce the shape of the J/ψ p_\perp and z distributions. The normalization is, however, off by a large factor. The value of the K factor is fairly large, of the order of 4 to 5 (depending on the experiment) when using the lowest-order expression for the leptonic decay width [4, 6, 8, 10]. Including QCD radiative corrections, the K factor is reduced by a factor of 2. The next-to-leading-order corrections which might account for

the large K factor have not yet been calculated. Nevertheless, from the agreement of the CS model with the data in the region $z < 0.9$ ($z = E_{J/\psi}/E_\gamma$ in the lab. frame), one usually concludes that the K factor is constant and the Born cross section may be used to extract the gluon density. In the high- z region, there is an excess of events not explained by the CS model, even when a K factor is applied to fit the low- z region [4, 6, 8–10]. We shall show that these events can be attributed to J/ψ production via the DD process.

We compare inelastic J/ψ production in the CS model with diffractive J/ψ production as predicted by (16) in Fig. 4. For the CS model we used the gluon-density parametrization B1 of Ref. [14] and a constant K factor adjusted to the FTFS data, $K = 2.8$. The t distribution is shown for various values of M^2 , the invariant mass of the remaining hadronic system X in $\gamma + p \rightarrow J/\psi + X$. We find that the diffractive reaction decreases with increasing M^2 whereas the inelastic process shows the opposite behaviour. Moreover, there is a region where both contributions are of similar size. Separating both contributions by a cut in z and/or t results in discontinuous distributions for the sum. Instead we require that the two contributions smoothly match.

In Figs. 5a and b the distributions in M^2 and in the variable z are presented at $s = 200 \text{ GeV}^2$. The DD events populate the low-mass region whereas the inelastic events occur dominantly at large M^2 . Similarly, the z distribution peaks at large z and is falling fast as z decreases for DD production. In contrast, for inelastic J/ψ production the z distribution is much flatter. Both contributions match at $M^2 \sim 8 \text{ GeV}^2$ and $z \sim 0.95$. The slope of the z distribution for J/ψ production via the DD process increases with energy. We find that the transition between the DD process and inelastic J/ψ production occurs at $M^2 \sim 500 \text{ GeV}^2$ and $z \sim 0.99$ at $\sqrt{s} = 250 \text{ GeV}$. Thus we expect the validity region of the CS model to extend towards larger values of z as the c.m. energy rises. We can parametrize the phase-space region where inelastic and diffractive J/ψ production match by:

$$M^2 \sim 8 \left(\frac{s}{200 \text{ GeV}^2} \right)^{0.7} \text{ GeV}^2. \quad (18)$$

In Fig. 6 we compare the c.m. energy dependence of the various reactions, elastic, diffractive, and inelastic J/ψ photoproduction. The totally inelastic region and the DD region are separated according to (18). We can clearly see the increasing importance of the totally inelastic reaction as well as its strong dependence on the input gluon distribution. Finally we calculate J/ψ production rates for ep collisions at HERA, $\sqrt{s_{ep}} = 314 \text{ GeV}$, using the Weizsäcker-Williams approximation for the photon flux at the electron vertex. The Q^2 dependence of the photon-proton cross section we model by a dipole form factor $(1 + Q^2/m^2)^{-2}$, where we take $m = m_p$. Then we expect the following cross sections: $\sigma^{\text{el}} = 4.5 \text{ nb}$, $\sigma^{\text{DD}} = 1.4 \text{ nb}$, and $\sigma^{\text{inel}} = 8.3 \text{ nb}$. The last value was calculated within the CS model using the gluon distribution B1 of Ref. [14] and a constant K factor, $K = 2.8$, adjusted to the FTFS data.

In conclusion, we have modelled elastic and diffractive photoproduction of J/ψ using single-pomeron exchange and vector-meson dominance. With only one free parameter we obtain definite predictions for the c.m. energy dependence as well as for the differential distributions of J/ψ photoproduction. Measurements of these distributions are sensitive probes of the underlying physical picture. The t distributions of both elastic and diffractive J/ψ photoproduction are in agreement with current data. Their rise with energy, however,

is weaker in our model than what seemed to be preferred by present data. Forthcoming measurements of J/ψ production at HERA are eagerly awaited. Adding our prediction for diffractive J/ψ production to inelastic production as given in the CS model, we can explain the excess of events observed at large z . Being able to describe the whole z distribution up to $z = 1$ makes us confident that inelastic J/ψ production can reliably be used to extract the gluon density of the proton.

Acknowledgments

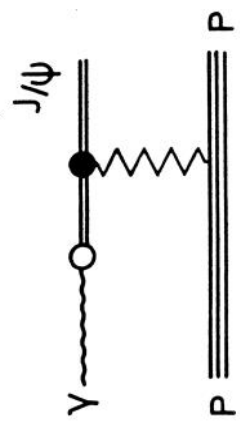
We want to thank F. Barreiro, H. Jung, P. Landshoff, M. Ryskin and D. Wyler for interesting discussions.

References

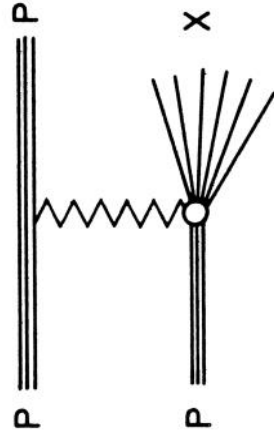
- [1] For a recent review, see e.g. P.V. Landshoff, CERN preprint CERN-TH.6277/91, Talk given at the LP-HEP '91 Conference, Geneva, 1991.
- [2] P.V. Landshoff and J.C. Polkinghorne, Nucl. Phys. B32 (1971) 541;
A. Donnachie and P.V. Landshoff, Phys. Lett. 123B (1983) 345;
A. Donnachie and P.V. Landshoff, Nucl. Phys. B231 (1984) 189.
- [3] a) G.A. Jaroszkiewicz and P.V. Landshoff, Phys. Rev. D10 (1974) 170;
b) A. Donnachie and P.V. Landshoff, Nucl. Phys. B244 (1984) 322;
c) A. Donnachie and P.V. Landshoff, Nucl. Phys. B267 (1986) 690.
- [4] FTPS Collaboration, B.H. Denby et al., Phys. Rev. Lett. 52 (1984) 795.
- [5] S.M. Tkaczyk et al., in Proc. Workshop on Physics at HERA, Hamburg, 1987, ed. R.D. Pececi, (DESY, Hamburg, 1988) p. 265;
H. Jung, G.A. Schuler and J. Tarron, to appear in Proc. Workshop on Physics at HERA, Hamburg, 1991, eds. W. Buchmüller and G. Ingelman.
- [6] NA14 Collaboration, R. Barate et al., Z. Phys. C33 (1987) 505.
- [7] IF Collaboration, M. Binkley et al., Phys. Rev. Lett. 48 (1982) 73.
- [8] BFP Collaboration, M. Strovink., Proc. 10th. Int. Symp. on Lepton and Photon Interactions at High Energies, Bonn, 1981. pp. 703-729.
- [9] EMC Collaboration, J.J. Aubert et al., Phys. Lett. 89B (1980) 267; Nucl. Phys. B213 (1983) 1; Phys. Lett. 152B (1985) 433.
- [10] NMC Collaboration, D. Allasia et al., Phys. Lett. B258 (1991) 493;
M. de Jong (NMC Collaboration), PhD Thesis, Utrecht (1991).
- [11] E.L. Berger and D. Jones, Phys. Rev. D23 (1981) 1521.
- [12] J.J. Hernandez et al., Rev. Part. Prop., Phys. Lett. B239 (1990) 1.
- [13] V.A. Novikov et al., Phys. Rep. C41 (1978) 1.
- [14] J.G. Morfin and Wu-Ki Tung, Z. Phys. C52 (1991) 13.

Figure captions

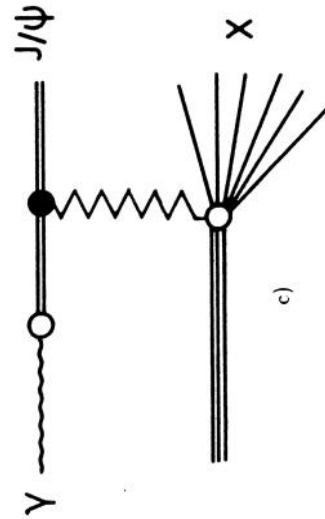
- Figure 1 Schematic diagrams for (a) elastic photoproduction of J/ψ mesons from proton targets, (b) diffractive dissociation of the proton in the reaction $pp \rightarrow pX$, and (c) photoproduction of J/ψ mesons in diffractive dissociation of the proton.
- Figure 2 The t distributions for photoproduction of J/ψ at $s = 200 \text{ GeV}^2$: elastic (solid), proton diffractive dissociation (dotted), and sum (dashed).
- Figure 3 Cross section versus c.m. energy for the sum of elastic and diffractive (DD) photoproduction of J/ψ . FTPS [4] forward elastic data in circles; NA14 [6] elastic data in open squares; BFP [8] ECAL $> 5 \text{ GeV}$ data in full squares; EMC citeEMC80 $z \geq 0.95$ data in triangles; dashed line: fit of IF [7] to their elastic plus diffractive target dissociation data (a 20% uncertainty should be added); dash-dotted line: fit of NMC [10] to their $z \geq 0.9$ data; model predictions as solid lines, from bottom to top: elastic (5), DD (16) and their sum.
- Figure 4 Double differential cross section $d\sigma/dt/dM^2$ of photoproduction of J/ψ at $s = 200 \text{ GeV}^2$: DD production (16) in dots for $M^2 = 3, 5, 7$, and 9 GeV^2 from top to bottom; inelastic production in the CS model (gluon parametrization B1 of Ref. [14] and $K = 2.8$) as solid lines for $M^2 = 9, 11, 13, 15, 17$, and 19 GeV^2 from bottom to top.
- Figure 5 Distributions in M^2 (a) and z (b) for the sum of DD J/ψ photoproduction (16) and inelastic J/ψ production in the CS model (gluon parametrization B1 of Ref. [14] and $K = 2.8$) at $s = 200 \text{ GeV}^2$.
- Figure 6 Centre-of-mass energy dependence of the various contributions to photoproduction of J/ψ : elastic (5) in dashes, DD (16) as solid line, inelastic production in the CS model ($K = 2.8$) in dots for set B1 of Ref. [14] and in dash-dots for set B2.



a)



b)



c)

Figure 1:

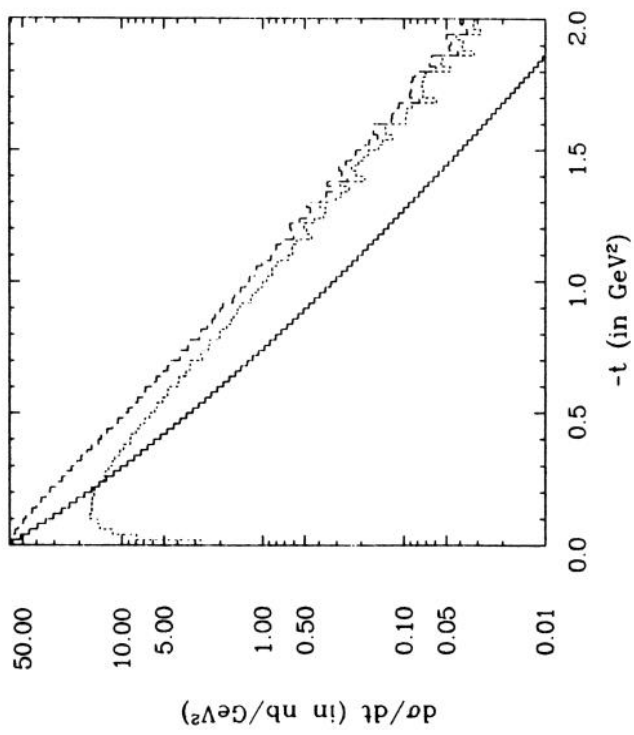


Figure 2:

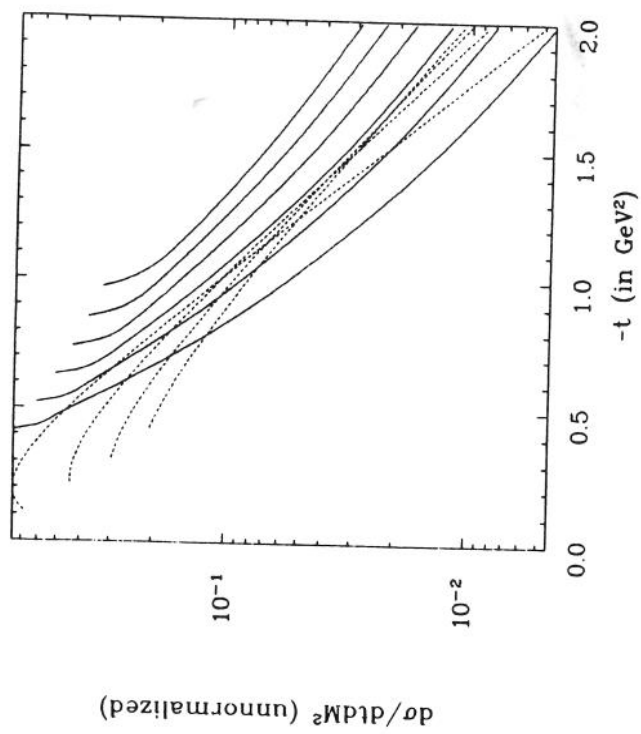


Figure 4:

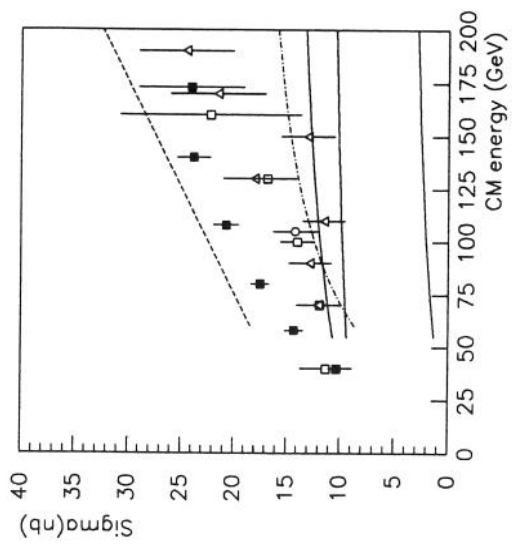


Figure 3:

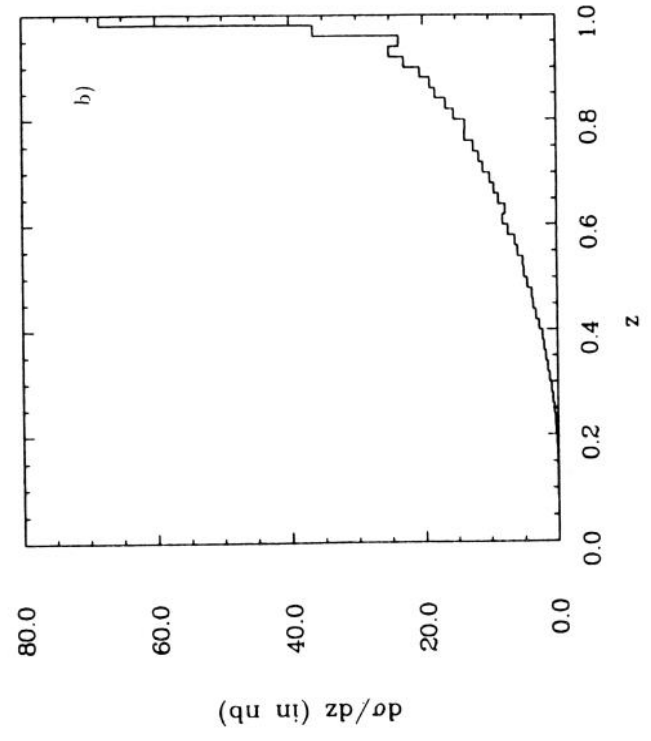
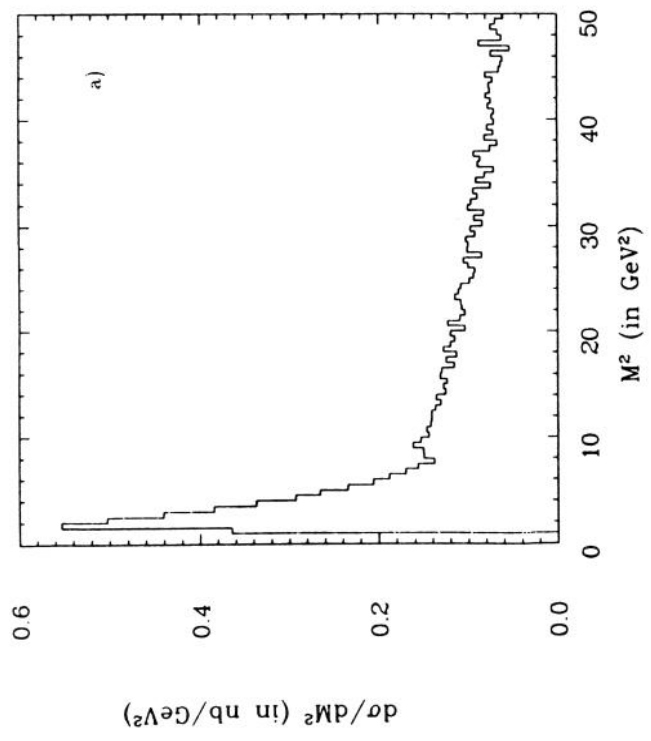


Figure 5:

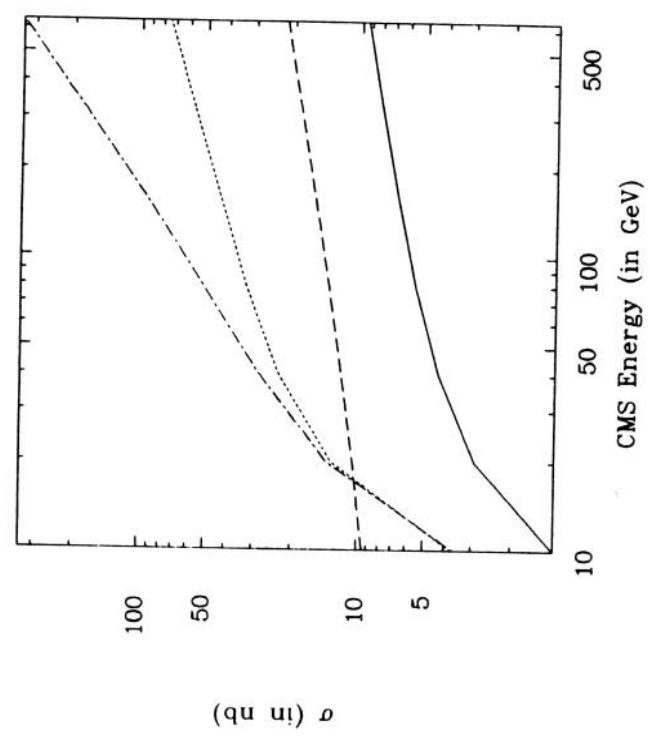


Figure 6: